JACS
JOURNAL OF THE AMERICAN CHEMICAL SOCIETY
Article
pubs.acs.org/JACS
Terms of Use

Zwitterionic Poly(amino acid methacrylate) Brushes

Abdullah M. Alswieleh,[†] Nan Cheng,[†] Irene Canton,[‡] Burcin Ustbas,[‡] Xuan Xue,[†] Vincent Ladmiral,[†,∥] Sijing Xia,[†] Robert E. Ducker,[†] Osama El Zubir,[†] Michael L. Cartron,[§] C. Neil Hunter,[§] Graham J. Leggett,*[,†] and Steven P. Armes*[,†]

[†]Department of Chemistry, University of Sheffield, Brook Hill, Sheffield S3 7HF, United Kingdom
[‡]Department of Biomedical Science, The University of Sheffield, Western Bank, Sheffield S10 2TN, United Kingdom
[§]Department of Molecular Biology and Biotechnology, University of Sheffield, Western Bank, Sheffield S10 2TN, United Kingdom

Supporting Information

ABSTRACT: A new cysteine-based methacrylic monomer (CysMA) was conveniently synthesized via selective thia-Michael addition of a commercially available methacrylate-acrylate precursor in aqueous solution without recourse to protecting group chemistry. Poly(cysteine methacrylate) (PCysMA) brushes were grown from the surface of silicon wafers by atom-transfer radical polymerization. Brush thicknesses of ca. 27 nm were achieved within 270 min at 20 °C. Each CysMA residue comprises a primary amine and a carboxylic acid. Surface zeta potential and atomic force microscopy (AFM) studies of the pH-responsive PCysMA brushes confirm that they are highly extended either below pH 2 or above pH 9.5, since they possess either cationic or anionic character, respectively. At intermediate pH, PCysMA brushes are zwitterionic. At physiological pH, they exhibit excellent resistance to biofouling and negligible cytotoxicity. PCysMA brushes undergo photodegradation: AFM topographical imaging indicates significant mass loss from the brush layer, while XPS studies confirm that exposure to UV radiation produces surface aldehyde sites that can be subsequently derivatized with amines. UV exposure using a photomask yielded sharp, well-defined micropatterned PCysMA brushes functionalized with aldehyde groups that enable conjugation to green fluorescent protein (GFP). Nanopatterned PCysMA brushes were obtained using interference lithography, and confocal microscopy again confirmed the selective conjugation of GFP. Finally, PCysMA undergoes complex base-catalyzed degradation in alkaline solution, leading to the elimination of several small molecules. However, good long-term chemical stability was observed when PCysMA brushes were immersed in aqueous solution at physiological pH.

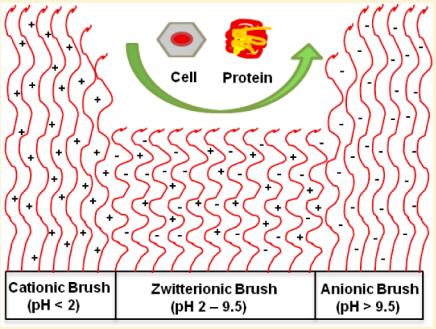

INTRODUCTION

There is considerable academic and commercial interest in the design of biocompatible nonfouling surfaces for biological fluids, particularly blood plasma and serum.[1,2] Protein fouling can damage biomedical devices, including coronary stents,[3] ear grommets,[4] and guide wires;[5] it may also compromise the performance of biosensors,[6] induce opsonization, and trigger clearance of nanocarriers from the bloodstream.[7] Adsorbed proteins increase the bioburden for both external[8] and intraocular[9] contact lenses, and play a critical role in thrombus formation in cardiovascular implants.[10] Nonfouling surfaces are important in biosensors, and in fundamental studies of biomaterial interfaces, because for recognition-based binding of analytes, it is first necessary to eliminate nonspecific binding. In array-based biosensors, nonfouling surfaces must be capable of modification to yield spatially selective binding of probe molecules.

Poly(ethylene glycol) (PEG)-based surface coatings are known to offer high resistance toward nonspecific protein adsorption and cell adhesion.[11] However, PEG-based materials can be oxidized under physiological conditions,[12] which can lead to activation of complement responses.[13] Over the past decade or so, much research activity has been focused on the design of alternative nonfouling biomaterials, which has led to considerable advances in the design of novel biocompatible materials. Various new surface coatings, such as self-assembled monolayers (SAMs), grafted polymer layers, and polymer brushes,[14−16] have been proposed that substantially reduce protein absorption.

Polymer brushes are polymer chains that are tethered to either a planar or a colloidal surface, usually via just one chain-end. The most effective strategy for the synthesis of well-defined polymer brushes is the so-called "grafting from" approach.[17,18] Many controlled/living polymerization techniques (CLP), including living anionic/cationic polymerization, nitroxide-mediated polymerization (NMP),[19] and reversible addition−fragmentation chain transfer (RAFT) polymerization,[20] have been utilized for the chain growth reaction.[21] Arguably the most popular formulation is based on atom transfer radical polymerization (ATRP).[22,23] This approach has been exploited to prepare a wide range of functional polymer brushes from many types of surfaces, including gold, silica, mica, base metals, etc.[17,24−27]

Received: April 9, 2014
Published: June 2, 2014

   dx.doi.org/10.1021/ja503400r | J. Am. Chem. Soc. 2014, 136, 9404−9413

Scheme 1. (A) Synthesis of the Cysteine Methacrylate Monomer (CysMA) Used in This Work and (B) Synthesis of a PCysMA Brush from this Initiator-Functionalized Planar Surface via Atom Transfer Radical Polymerization (ATRP) in Deionized Water at 20°C Using a Copper-Based Catalyst

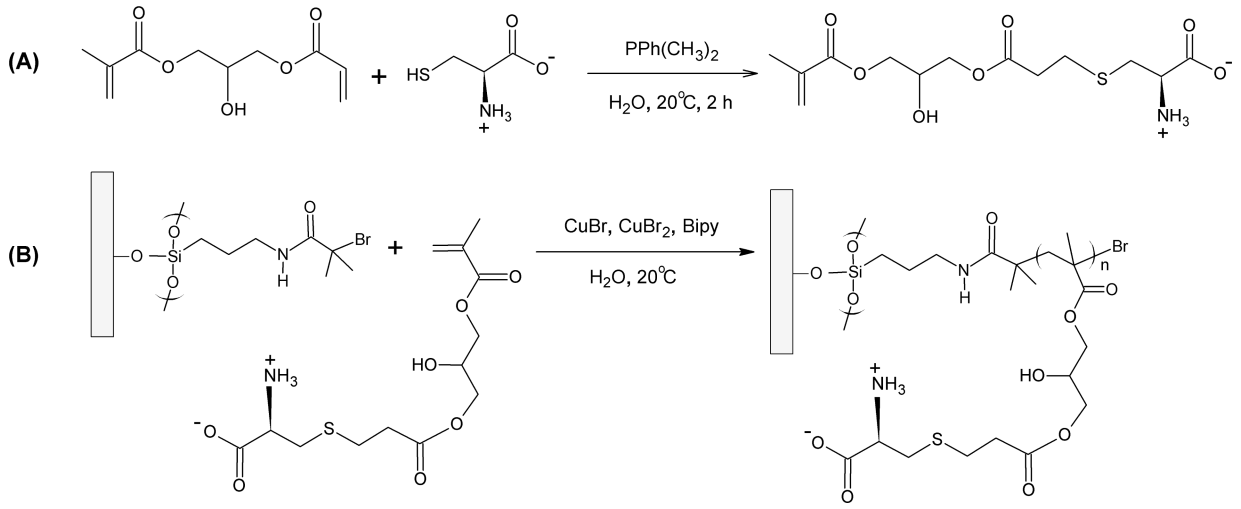

Poly[oligo(ethylene glycol) methacrylate] (POEGMA) brushes exhibit exceptional resistance to protein adsorption from blood serum, and also cell adhesion.[28,29] For example, Katira et al. found that adsorption of kinesin onto a 50 nm POEGMA brush was 20 times lower than that found for monohydroxy-capped (triethylene glycol)-terminated SAM surfaces.

Particular attention has been paid to *stimulus-responsive* polymer brushes based on either polyacids or polybases.[30−32] These polyelectrolytic brushes are typically responsive to changes in pH or ionic strength.[32−34] For example, the stimulus-responsive behavior of poly(acrylic acid) brushes has been studied by Ayres et al.[35] Collapsed brushes were observed below the pK_a of the brush, whereas highly anionic swollen brushes were formed above this critical value.[35] The pH-responsive behavior of poly(methacrylic acid) brushes, which enable switching between collapsed and stretched brush conformations at different pH, has been investigated using ellipsometry and atomic force microscopy (AFM).[36] Complementary behavior has been reported for various weak polybase brushes based on either poly(2-(diethylamino)ethyl methacrylate) (PDEAEMA),[30] or poly(2-(dimethylamino)ethyl methacrylate) (PDMA).[31,37]

Polymers containing zwitterionic structural units have been used for a wide range of biomedical and engineering applications. Such surface coatings are highly resistant to nonspecific protein adsorption, bacterial adhesion, and biofilm formation.[6,38] Jiang and co-workers have demonstrated that glass slides grafted with two zwitterionic polymers, poly(sulfobetaine methacrylate) (PSBMA) and poly(carboxybetaine methacrylate) (PCBMA), exhibit exceptional resistance to fouling.[39] In some cases the zwitterionic character is insensitive to the solution pH (e.g., poly(sulfobetaine methacrylate) (PSBMA),[40] and poly(2-(methacryloyloxy)ethyl phosphorylcholine) (PMPC)[41]), whereas in other cases pH-sensitivity can be observed. For example, zwitterionic poly(carboxybetaine methacrylate) brushes exhibit zwitterionic character at neutral pH, but cationic polyelectrolytic character at low pH.[42]

As far as we are aware, there has been relatively little work focused on polymers containing amino acid motifs as side-chains.[43,44] For example, Rosen et al. reported that cysteine-functionalized silica nanoparticles resisted protein fouling when challenged with either lysozyme or bovine serum albumin (BSA).[45] Azzaroni and co-workers grew cationic poly(methacryloyl-L-lysine) brushes from mesoporous silica using surface-initiated radical polymerization with the aim of modulating ionic transport via pH variation.[43] Liu et al. prepared zwitterionic poly(serine methacrylate) (PSerMA) brushes on a planar gold substrate using surface-initiated photoiniferter-mediated polymerization (SI-PIMP) for evaluation as a potential antibiofouling material.[44] Very recently, Jiang and co-workers have reported the synthesis of new polycarboxybetaine brushes based on two new amino-acid-based methacrylic monomers prepared via three-step and five-step protocols, respectively.[46]

Herein a new zwitterionic monomer, cysteine methacrylate (CysMA), has been conveniently synthesized via thia-Michael addition of cysteine to a commercial methacrylate-acrylate precursor (see Scheme 1A). This facile synthesis is particularly noteworthy because it is conducted on *a multigram scale in aqueous solution without recourse to protecting group chemistry*. This offers the promise of greatly reduced cost compared to other zwitterionic polymer brush systems such as PMPC. SI-ATRP was then used to grow PCysMA brushes from planar silicon wafers (see Scheme 1B), and their stimulus-responsive behavior with respect to changes in pH and ionic strength was investigated using ellipsometry, atomic force microscopy (AFM), and surface zeta potential measurements. Micro- and nanopatterned PCysMA brushes were prepared via UV irradiation using a photomask and interference lithography (IL), respectively. Selective adsorption of fluorescent proteins on these model surfaces was characterized by confocal fluorescence microscopy. The long-term aqueous chemical stability of PCysMA brushes immersed in alkaline media and the UV-induced photodegradation of dry PCysMA brushes was examined using X-ray photoelectron spectroscopy (XPS) and AFM. Finally, complement depletion assays were used to compare the antibiofouling performance of PCysMA brushes to other well-known biocompatible PMPC and POEGMA brushes.

dx.doi.org/10.1021/ja503400r | J. Am. Chem. Soc. 2014, 136, 9404−9413

RESULTS AND DISCUSSION

Preparation of CysMA monomer. Cysteine methacrylate (CysMA) monomer was synthesized at 20 °C in aqueous solution by a selective thia-Michael addition.[47] A natural amino acid, L-cysteine, was reacted with 3-(acryloyloxy)-2-hydroxypropyl methacrylate in the presence of a nucleophile catalyst (DMPP), see Scheme 1A. Thia-Michael addition proved to be relatively efficient, with an overall yield of 94% being achieved within 2 h. The chemical structure of the purified monomer was confirmed by ^{1}H and ^{13}C NMR spectroscopy, mass spectroscopy and elemental microanalyses (see Supporting Information).

Growth of PCysMA brushes from BIBB-APTES film. Films formed by the adsorption of 3-aminopropyl triethoxysilane (APTES) onto silica were reacted with 2-bromoisobutyryl bromide (BIBB) to generate 3-(2-bromoisobutyramido)-propyl triethoxysilane (BIBB-APTES).[48] The expected chemical composition of BIBB-APTES was confirmed by XPS studies (C 1s, Br 3d and N 1s core-line spectra), and the surface zeta potential of BIBB-APTES film was measured at different pH solution (Figures S2 and S3, see Supporting Information).

PCysMA brushes were grown from BIBB-APTES-functionalized silicon wafers via SI-ATRP, which is known to be an effective and convenient technique for the synthesis of dense uniform polymer brushes with controlled thickness (see Scheme 1B). The Cu(I)/Cu(II) molar ratio, solvent type, and CysMA/catalyst molar ratio in the aqueous ATRP formulation were varied so as to optimize the brush growth conditions. Figure 1 shows the evolution of PCysMA brush thickness over time at 20 °C using [CysMA]/[Cu(I)Br] molar ratios of 30, 100, and 150. Ellipsometric dry brush thicknesses of up to 27 ± 3 nm were achieved after 270 min. The brush thickness increased approximately linearly up to ca. 120 min, at which point there was a reduction in the rate of growth. Higher [CysMA]/[Cu(I)Br] molar ratios led to thicker PCysMA brushes, as expected.

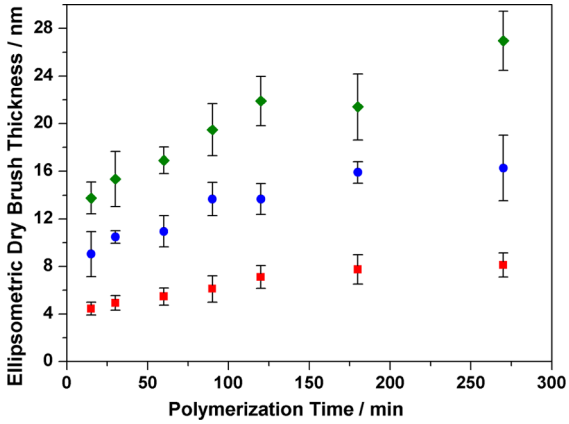

Figure 1. Evolution in ellipsometric dry brush thickness with polymerization time for the synthesis of PCysMA brushes via surface-initiated ATRP in deionized water at 20 °C. Conditions: (red squares) [CysMA]:[CuBr]:[$CuBr_2$]:[Bipy] molar ratio = 30:1.0:0.5:3; (blue circles) [CysMA]:[CuBr]:[$CuBr_2$]:[Bipy] molar ratio = 100:1.0:0.5:3; (green diamonds) [CysMA]:[CuBr]:[$CuBr_2$]:[Bipy] molar ratio = 150:1.0:0.5:3.

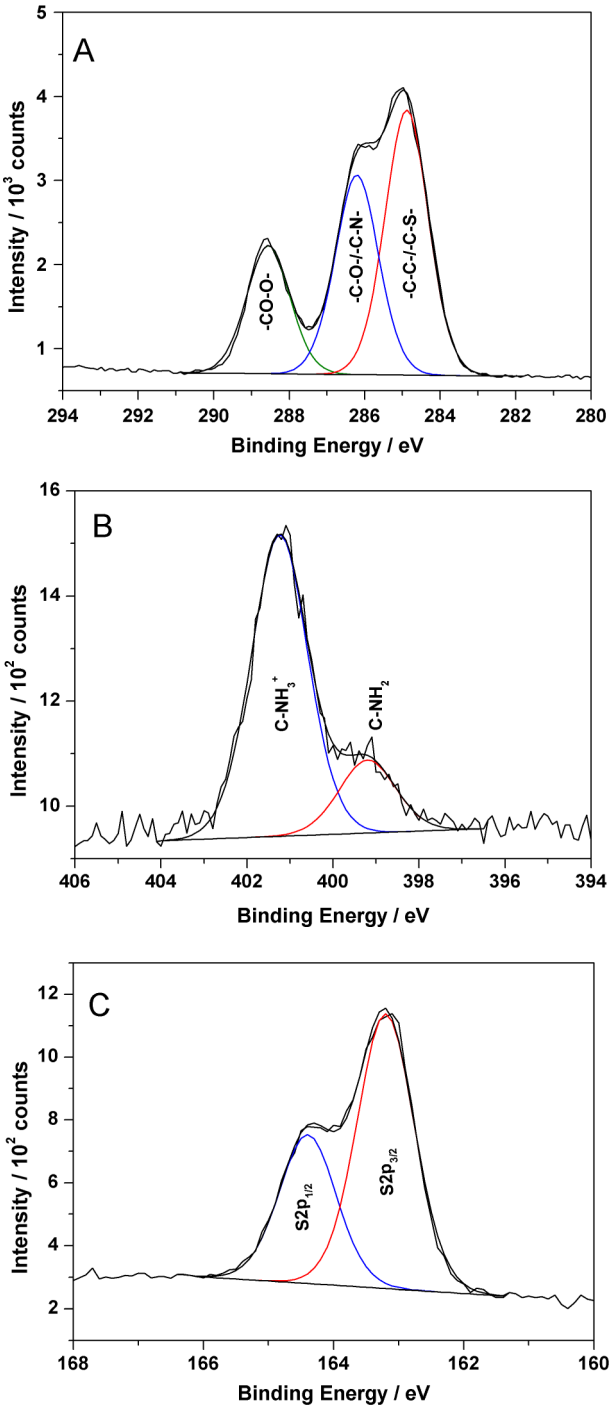

Figure 2. High resolution X-ray photoelectron spectra recorded for a PCysMA brush of 12 nm dry thickness: (A) C 1s spectrum, (B) N 1s spectrum, (C) S 2p spectrum.

High resolution C 1s, N 1s, and S 2p XPS spectra were acquired for PCysMA dry brushes in order to confirm their chemical structure (see Figure 2). XPS C 1s spectra were fitted using three components with binding energies of 285.0, 286.3, and 288.7 eV, which correspond to *C*—C, *C*—O/*C*—N, and O=*C*—O, respectively. The *C*—C, *C*—O/*C*—N, and O=*C*—O atomic ratios calculated from the fitted C 1s spectrum were 2:1.5:1, which is close to the theoretical ratio of 2:1.3:1. The binding energy of the O=*C*—O component was reduced by ca. 0.6 eV compared to the expected value for a carboxylic acid, consistent with previous reports for anionic carboxylate carbon atoms.[49] The N 1s core-line spectrum recorded for the PCysMA brush (dried at pH 6) was fitted using two

dx.doi.org/10.1021/ja503400r | J. Am. Chem. Soc. 2014, 136, 9404−9413

components centered at 399.0 and 401.5 eV, which correspond to C—NH_2 and C—NH_3^+ species.[50] It is estimated that about 80% of the surface primary amine groups are protonated. The high resolution S 2p spectrum was fitted using two S $2p_{3/2}$ and S $2p_{1/2}$ components with binding energies of 163.5 and 164.5 eV, respectively. The relative intensities of these components is approximately 2:1, as expected for $2J + 1$ spin−orbit coupling.[50]

Tapping mode AFM topographical images were acquired for PCysMA brushes both in the dry state and also immersed in PBS (see Figure S4, Supporting Information). The root-mean-square (rms) surface roughness averaged across the entire image area was 0.5 ± 0.2 nm in the dry state. However, the PCysMA brush became somewhat smoother when immersed in PBS solution, with an rms roughness of approximately 0.3 ± 0.1 nm.

pH-Responsive Behavior of PCysMA Brushes. The carboxylic acid and amine groups in each CysMA residue confer pH-responsive behavior on the PCysMA brushes. In this sense, these weak polyacid/weak polybase brushes differ significantly from permanently zwitterionic betaine-based brushes such as PMPC or PSBMA, or indeed PCBMA (which only possesses weak polyacid character). This complex pH-sensitive behavior was studied using both ellipsometry and AFM.

The pH-modulated dimensions of a PCysMA brush (dry brush thickness = 15 nm) immersed in an aqueous solution were investigated by varying the solution pH over a wide range. To enable the brush thickness to be measured by atomic force microscopy, patterned samples were prepared by UV irradiation of BIBB-APTES films through a mask. In exposed regions the bromine is removed from the initiator by photolysis of the C−Br bond. The initiator remains intact in the masked areas, from which brushes may be grown subsequently by ATRP.[48,51] The Br 3d signal in the XPS spectrum was found to decrease in intensity with UV exposure and became undetectable after a dose of 2.2 J cm^{-2}. In the present study, BIBB-APTES films were exposed to the same dose using a 2000 mesh electron microscopy grid as a photomask to generate a micropatterned BIBB-APTES monolayer, which was subsequently utilized to grow micropatterned PCysMA brushes by ATRP. The initial micropatterned substrate did not exhibit any height contrast between the UV-exposed and unexposed areas. Figure 3 shows an AFM topographical image acquired after ATRP had been carried out. Significant height differences were observed between irradiated areas (squares) and nonirradiated areas (bars), as expected (Figure 3). These height differences were quantified to determine the mean PCysMA brush thickness.

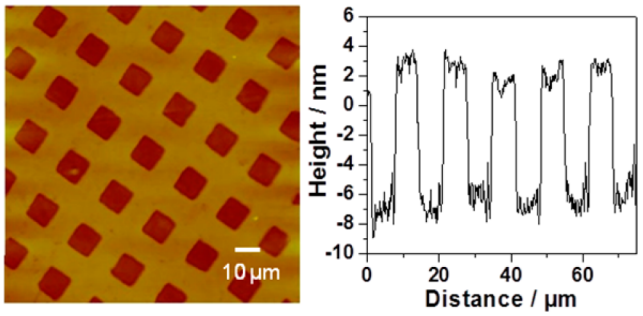

Figure 3. Tapping-mode AFM of the periodic brush height recorded for a micropatterned PCysMA brush: topographical image (left), cross section analysis (right). Image size: 75 × 75 μm^2, Z-range 0−50 nm.

The ellipsometric data (see Figure 4A) indicate that the PCysMA brushes become protonated at a pH less than ca. 2.0

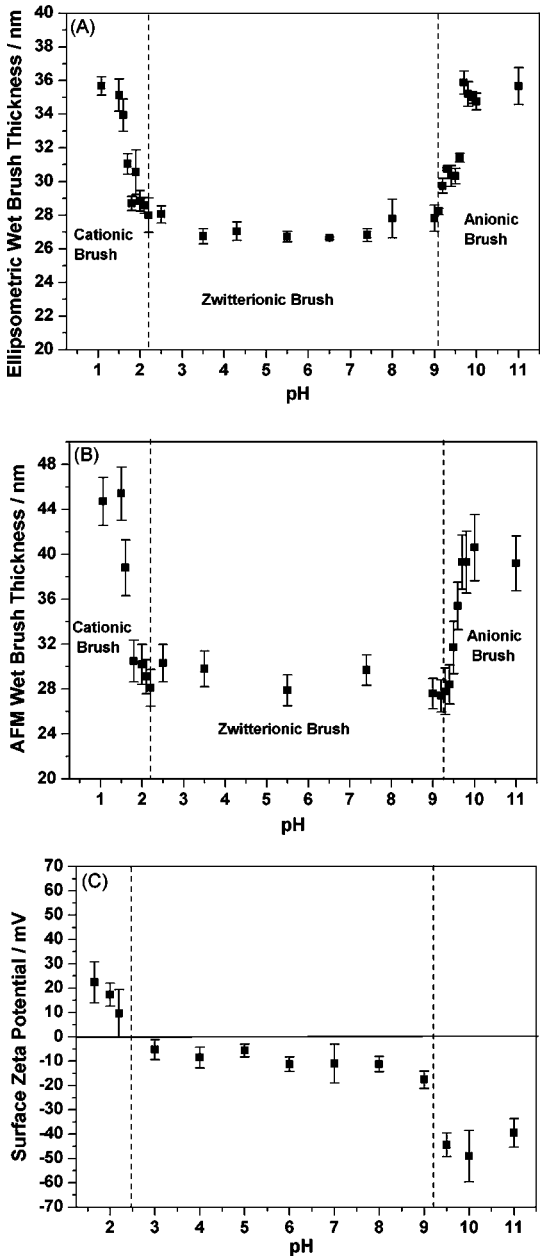

Figure 4. Variation in the *in situ* brush thickness with pH for a PCysMA brush of 15 nm dry thickness immersed in aqueous solution by (A) ellipsometry and (B) AFM. (C) Surface zeta potential vs pH curves obtained for PCysMA brushes using a Malvern dip cell. PCysMA brush (original dry brush thickness = 22 nm) immersed in aqueous solutions of varying pH in the presence of 1 mM KCl as background electrolyte.

and attain their maximum swollen thickness at a pH of ca. 1.5. Below its pK_a, the carboxylic acid group is no longer ionized, while all the amine groups remain protonated. Thus the brush layer stretches away from the surface because of the strong lateral electrostatic repulsion between adjacent cationic chains. In contrast, the amine groups become deprotonated above their pK_a while the carboxylic acid groups remain ionized; hence, the brushes acquire anionic character and hence become highly swollen above pH 9.8. The mean brush thickness increased

dx.doi.org/10.1021/ja503400r | J. Am. Chem. Soc. 2014, 136, 9404−9413

from 15 nm (dry state) to approximately 36 nm at pH 1.5. Between pH 1.6 and 2.0, there is a gradual reduction in brush thickness from 36 to 28 nm because of the higher degree of ionization of the carboxylic acid groups. The mean PCysMA brush thickness then remains constant at approximately 26 nm between pH 2.0 and pH 9.5; this corresponds to the zwitterionic brush regime. Finally, the brush thickness increases from 28 nm to approximately 34−35 nm between pH 9.5 and pH 9.8 as the amine groups become deprotonated and the brush chains acquire anionic character. In summary, the PCysMA brushes exhibit zwitterionic character at intermediate pH values (i.e., pK_a^{COOH} < pH < $pK_a^{NH_2}$) and are somewhat less swollen than their polyelectrolytic forms under these conditions.

Measurements were made by AFM on a micropatterned PCysMA brush, similar to the one shown in Figure 3, immersed in aqueous solutions of varying pH. The height difference was measured between the brush-functionalized bars and the square regions from which the initiator was removed by UV exposure. Figure 4B shows the change in brush height as a function of pH. The brush height increases from about 15 nm in the dry state to 44 nm when immersed in an acidic solution (pH < 1.5). The brush height is gradually reduced between pH 1.6 and 2.0, and then remains constant at approximately 28 nm between pH 2.0 and 9.5. Finally, there is a gradual increase in brush height between pH 9.5 and 9.7, and a maximum brush thickness of 40 nm is observed above pH 10. The pK_a of the carboxylic acid groups in the PCysMA brush is estimated to be approximately 1.7, compared to a pK_a of 2.0 for the carboxylic acid group of L-cysteine. Similarly, the amine pK_a of the PCysMA brushes is estimated to be 9.6, whereas it is reported to be 10.2 for L-cysteine.[52] These differences are attributed to the well-known polyelectrolyte effect: the pH response of polyacids and polybases is always weaker than the corresponding small molecules, since polymer chains tend to resist the build-up of local charge density.[53]

These AFM observations are in generally good agreement with the ellipsometric data, with minor differences most likely arising because of uncertainties in the refractive index of 1.50 estimated for the PCysMA brush when modeling the ellipsometric data (N.B. this parameter is also likely to vary with the solution pH).

There has recently been interest in the use of pH-responsive polymers for various applications, for example for gating channels[54] or, more recently, for the reversible trapping and release of nanoparticles or proteins.[46] PCysMA is an attractive material for such applications because of the facile monomer synthesis and the unusual pH-responsive properties of the polymer.

The determination of surface zeta potentials for planar surfaces has been recently described using a new commercial dip cell developed by Malvern Instruments.[55] However, as far as we are aware, this technique has only recently applied to characterize pH-responsive polymer brushes.[51] Surface zeta potentials were determined for PCysMA brushes over a wide range of solution pH, see Figure 4C. Positive surface zeta potentials of +15 ± 5 mV were observed below pH 2 for protonated PCysMA brushes. Between pH 2.5 and 9.0, the PCysMA brush exhibited weakly negative surface zeta potentials (−5 to −10 mV). In principle, the brush layer should be in its zwitterionic form over this pH range, so zero surface zeta potentials might be expected. The observed weakly anionic character may indicate preferential adsorption of Cl^- and/or OH^- from the bulk solution. Above pH 9, the surface zeta potential becomes much more negative (−40 ± 8 mV), indicating deprotonation of the amine groups within the PCysMA brush. Overall, these surface zeta potential data are consistent with the changes in brush thickness observed using ellipsometry and AFM discussed above and support our interpretation of the complex pH-modulated behavior exhibited by this doubly pH-responsive brush in aqueous solution.

PCysMA brushes exhibited good chemical stability in either acidic or neutral aqueous solution. However, degradation was observed under basic conditions. Ellipsometric studies indicate a gradual reduction in brush thickness from 10 to 7 nm at pH 9 (see Figure S5, Supporting Information). At pH 10, the mean brush thickness is reduced from 10 to 3 nm within 48 h. Finally, a brush thickness of just 1.5 nm is observed within 24 h at pH 11. In contrast, no discernible change in the ellipsometric brush thickness is observed after 9 days at pH 8. Thus it seems that, although these brushes are susceptible to base-catalyzed hydrolysis, they nevertheless possess sufficient stability under physiological conditions to be considered for biomedical applications. There are at least four possible degradation pathways. In principle, a primary amine group could react intramolecularly with an ester carbonyl that is located either on the same CysMA residue or on an adjacent repeat unit to form an amide. If the primary amine group reacts with an ester carbonyl on a neighboring PCysMA chain, a cross-link can be formed. At higher pH, base-catalyzed ester hydrolysis is also likely to occur.

No changes are observed in the X-ray photoelectron spectra recorded for PCysMA brushes after their immersion in an aqueous solution at pH 8 for 48 h. However, exposing PCysMA brushes to alkaline media (pH > 9) led to various spectroscopic changes over this time scale (Figure S6, see Supporting Information). A significant reduction in the C 1s intensity is observed, which indicates substantial mass loss and implies chemical degradation. The S 2p and N 1s signals each become attenuated over time, indicating loss of the cysteine fragment from the brush layer. However, it is emphasized that there is no evidence for chemical degradation at neutral pH, which suggests that this new zwitterionic PCysMA brush may offer potential applications as a surface coating under physiological conditions.

Salt-Responsive Behavior. The effect of ionic strength on the PCyMA brush dimensions was also investigated by adding salt (NaCl). According to the literature, polybetaines such as PCysMA are expected to expand on addition of salt.[56] Such behavior is known as the "antipolyelectrolyte" effect. Figure 5 shows the change in PCysMA brush thickness in the presence of added salt at pH 6, as judged by ellipsometry. The mean brush thickness increased monotonically from 28.0 to 30.5 nm when immersed in aqueous solutions containing 0.3 to 1.5 M NaCl. The salt screens the interchain *attractive* electrostatic interactions, which allows modest brush expansion. In contrast, the addition of salt to polyelectrolytes screens the *repulsive* electrostatic interactions between adjacent chains, leading to their collapse (see Figure 5). Thus, at pH 1.5, there is a gradual reduction in the wet *cationic* brush thickness from 43 to 35 nm on addition of salt. Similar behavior is observed when salt is added to *anionic* PCysMA brushes at pH 9.8: the ellipsometric wet brush thickness is reduced from 48 to 35 nm in the presence of 1 M NaCl.

Photodegradation and Photopatterning of PCysMA Brushes. PCysMA brushes grown from silicon wafers were

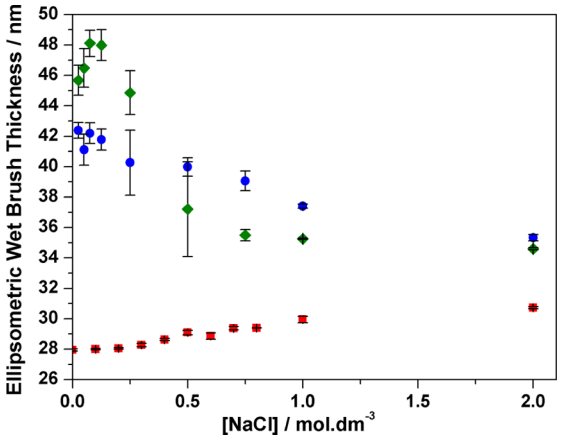

Figure 5. *In situ* ellipsometric wet thickness of PCysMA brushes as a function of added salt at 20 °C. Red squares: immersed in aqueous solution at pH 6, original dry thickness 15 nm. Blue circles: immersed in aqueous solution at pH 1.5, original dry thickness 18 nm. Green diamonds: immersed in aqueous solution at pH 9.8, original dry thickness 18 nm.

subjected to various UV doses at 244 nm. Significant changes were observed in the C 1s spectra during this irradiation (Figure 6A). In particular, there is a systematic reduction in the C 1s signal intensity with longer exposure times (5 min), which suggests that the brush thickness is reduced with increasing UV exposure. Moreover, a new component is observed at ~288 eV which is assigned to the formation of surface aldehyde groups.

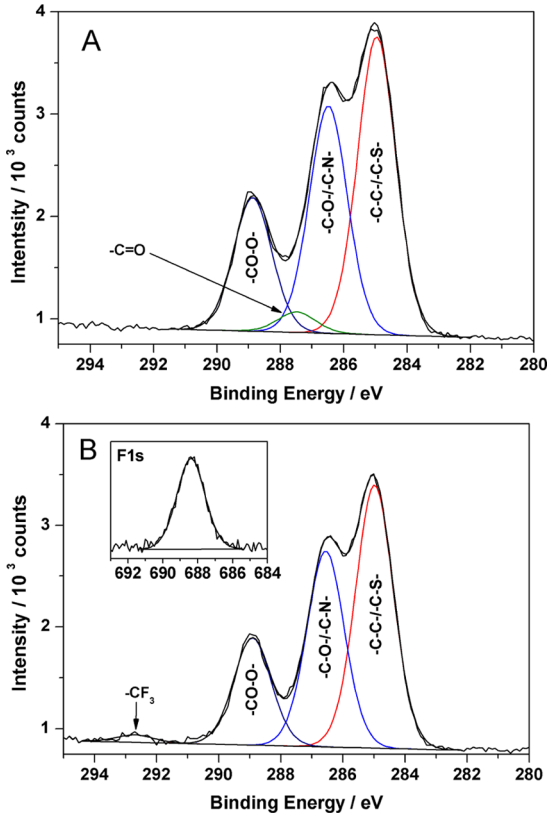

Figure 6. (A) Peak-fitted C 1s spectrum of PCysMA brush after UV irradiation (total dose 10.4 J cm^{-2}) including the aldehyde component at 288 eV. (B) C 1s and (inset) F 1s peak-fitted X-ray photoelectron spectra recorded for PCysMA brushes exposed to UV radiation (total dose = 48 J cm^{-2}) and subsequently immersed into an ethanolic solution of trifluoroethylamine.

These surface aldehyde groups were reacted with a perfluorinated primary amine to produce imine linkages via Schiff base chemistry; this is a well-known assay that has the advantage of enhancing the XPS sensitivity. Figure 6B shows the C 1s and F 1s spectra recorded for a PCysMA brush after an exposure of 14 J cm^{-2}, followed by immersion in an ethanolic solution of trifluoroethylamine. For the treated sample, the observation of a strong F 1s peak at 688.5 eV and a new component at ca. 293 eV in the C 1s region (assigned to the CF_3 unit in the amide product) provide good evidence that the reaction has taken place.

A uniform PCysMA brush-functionalized silicon wafer was exposed to UV radiation using a photomask and subsequently imaged using AFM (Figure 7). After exposure, the exposed regions (squares) exhibited reduced height compared to the masked regions (bars). As the exposure increased the height difference between the masked and exposed regions increased. After an exposure of 48 J cm^{-2}, the height difference was ca. 12 nm; thus the mean erosion rate was estimated to be 0.25 nm J^{-1} cm^2.

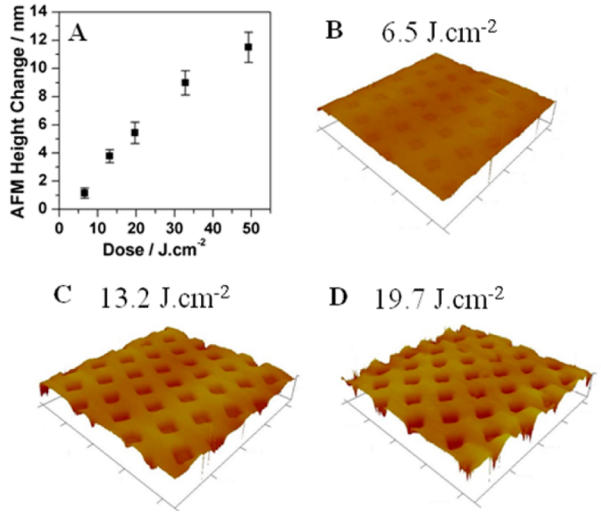

Figure 7. (A) Difference in height between masked and exposed areas as a function of dose for PCysMA brushes samples exposed to UV radiation (λ = 244 nm) through a mask (original dry brush thickness = 18 nm). Images B–D show 75 × 75 μm^2 AFM topographical images (with a common vertical range of 20 nm) as a function of UV dose.

Nanostructures were fabricated by photodegradation of a PCysMA brush using a dual-beam interferometer.[57] A coherent UV laser beam was directed toward a mirror, and the PCysMA brush-coated silicon wafer was placed at an angular separation of 2θ. Half of the laser beam fell on the mirror, from where it was reflected onto the sample to interfere with the other half of the beam, forming a pattern with a sinusoidal variation in intensity and a period of $\lambda/2\sin\theta$, where λ is the laser wavelength (244 nm). AFM images of the resulting structures are shown in the Supporting Information. The PCysMA brush was exposed to a UV dose of 13.2 J cm^{-2} at angles of 10°, 20°, 30°, and 45°, yielding PCysMA brush nanolines with mean line widths (full width at half-maximum, fwhm) of 350 ± 5 nm, 245 ± 5 nm, 130 ± 5 nm, and 100 ± 5 nm, respectively, and heights of 3 ± 1 nm, 3 ± 0.5 nm, 3 ± 0.5 nm, and 2 ± 0.5 nm, with

dx.doi.org/10.1021/ja503400r | J. Am. Chem. Soc. 2014, 136, 9404–9413

periods of 730 ± 20 nm, 455 ± 15 nm, 235 ± 15 nm, and 190 ± 10 nm, respectively.

Protein Patterning. PCysMA brushes exhibit excellent resistance toward protein adsorption, but this protein resistance was found to be lost after exposure to UV light. PCysMA brushes were subjected to UV irradiation using a photomask. They were then immersed in an aqueous solution containing 10 μg mL^{-1} GFP in PBS (see Figure 8A). In the masked areas

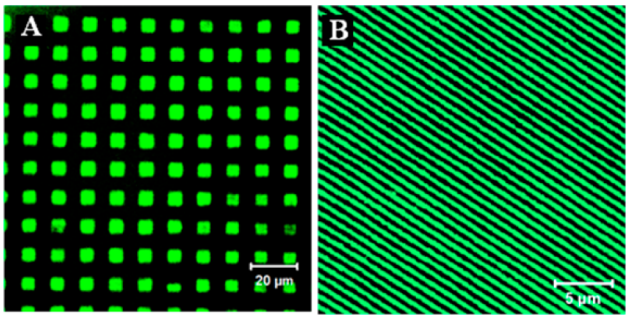

Figure 8. Confocal fluorescence images obtained for PCysMA brushes subjected to a green fluorescent protein (GFP) challenge: (A) GFP protein is immobilized within bright green squares after selective degradation of PCysMA using a photomask (dark areas represent the unexposed PCysMA brush); (B) green fluorescent protein (GFP) immobilized in nanopatterned lines after selective degradation of PCysMA using a two-beam interferometer at θ = 10°.

(bars in Figure 8A) no fluorescence can be detected within the limits of sensitivity, which indicates that the pristine PCysMA brush strongly resists protein adsorption. In contrast, strong green fluorescence is observed from the UV-irradiated square regions, indicating efficient selective GFP immobilization within these areas. Such a well-defined GFP pattern within a PCysMA brush (combined with minimal background fluorescence) suggests that this new photopatternable antibiofouling brush layer offers considerable potential for various biomedical applications. Control samples that had not been exposed to UV light (Supporting Information, Figure S8) exhibited no fluorescence.

Protein nanopatterns were fabricated by interferometric lithography (IL) (Figure 11B). A PCysMA brush (mean dry brush thickness = 15 nm) was exposed to a UV dose of 13.2 J cm^{-2} at an angle of 10°, and immersed in a 10 μg mL^{-1} solution of GFP in PBS. A relatively small angle was selected, leading to a comparatively large period and fwhm, to enable characterization of the structures by confocal microscopy, which is a diffraction-limited technique. The green lines indicate that GFP has adsorbed to the chemically modified brush chains, corresponding to regions that were exposed to maxima in the interferogram, whereas the unmodified brush regions (exposed to minima in the interferogram) continue to resist protein adsorption strongly. Individual lines are well-resolved, and the mean line width was estimated to be 350 nm.

For array-based biosensors, and for fundamental studies of interfacial biological phenomena, it is important to be able to introduce protein-binding regions into a protein-resistant surface. The data shown in Figure 8 exhibit high contrast between modified and unmodified regions, indicating that very effective control of protein−surface interactions is achieved with high spatial selectivity. Additionally, the protein-resistant PCysMA is converted to a protein-binding aldehyde functionality in a single step, in contrast to the multistep processes that are typically used to attach biomolecules to surfaces. This is a further significant advantage of this methodology.

Biocompatibility and Antibiofouling Assay. Many studies have assessed antibiofouling performance using single protein assays [i.e., HSA, fibrinogen, and single complement proteins (C3b)].[13] However, reduction of the absorption of a single blood plasma protein is insufficient evidence for stealth-like properties.[58] Perhaps surprisingly, there are relatively few literature reports that assess the antibiofouling performance of poly-zwitterion-based surface coatings utilizing full blood plasma.[59] In principle, antibiofouling assays that involve incubation with whole human serum (which contains a full set of complement proteins) and utilize cell membrane lysis as the end-point offer the potential for mimicking possible activation through all the known complement pathways.[60]

The cytotoxicity of these PCysMA brushes was evaluated using a biological assay (see Supporting Information). There was no evidence of cytotoxicity for human dermal fibroblasts exposed to PCysMA brushes over a wide range of brush thicknesses. The MTT assay was used to assess the extent of cell adhesion, which is a well-recognized requirement for cell viability of adherent cells such as fibroblasts.[61] An adhesion study was performed for 24 h in order to evaluate the antibiofouling performance of PCysMA brushes in conjunction with HDF cells. Over this time period, very few HDF cells adhered to the PCysMA brush-coated glass substrates (see Figure 9). Optical microscopy studies suggested that very few

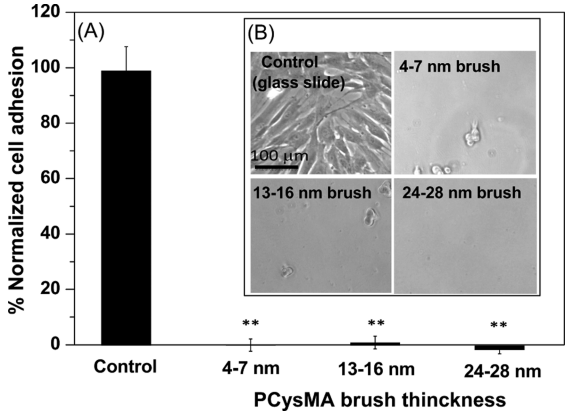

Figure 9. HDF cell adhesion onto PCysMA brushes. PCysMA brushes were grown from identical 13 mm diameter circular glass slides to examine the extent of cellular adhesion on these substrates. Uncoated glass slides were used as controls. Both PCysMA-coated and uncoated glass slides were disinfected using ice-cold ethanol and placed at the bottom of 24-well plates. HDFs cells were then added (1 × 10^5 cells per well), and cells were incubated for 24 h at 37 °C. (A) Cell adhesion onto three series of PCysMA brushes (with dry brush thicknesses of 4−7 nm, 13−16 nm, or 24−28 nm). Cell adhesion was determined via MTT assay. N = 3 independent experiments were performed in duplicate wells. **p < 0.01. (b) Optical micrographs obtained for HDF cells growing on the brush surfaces after 24 h incubation.

cells became attached to either the relatively short (4−7 nm) brushes or those of intermediate thickness (13−16 nm), while no adhering cells at all were observed for the relatively thick 24−28 nm brushes (Figure 9B). When surface attachment did occur, adhering cells exhibited a pseudospherical morphology (Figure 9B), whereas the control cells were both highly adherent and fully stretched. This indicates that the PCysMA

dx.doi.org/10.1021/ja503400r | J. Am. Chem. Soc. 2014, 136, 9404−9413

brushes strongly resist cell adhesion when immersed in culture media in the presence of HDF cells over an extended incubation period.

A complement depletion assay was utilized to further investigate the effect of varying the PCysMA brush thickness in the context of protein fouling (see Figure 10). On exposure

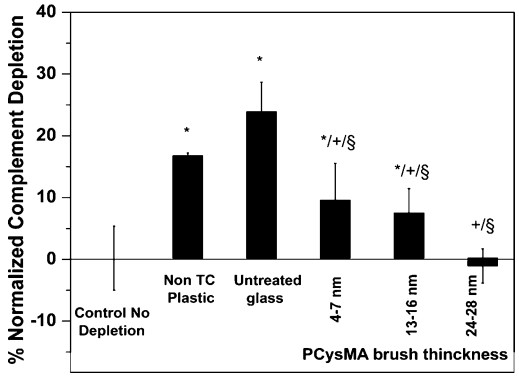

Figure 10. Complement depletion assays performed on PCysMA brushes of varying thickness. PCysMA brushes were grown from 13 mm diameter circular glass slides with mean dry brush thicknesses of 4−7 nm, 13−16 nm, and 24−28 nm and incubated with human serum (100 μL) for 1 h at 37 °C. Supernatants were then removed and mixed with fresh antibody-sensitized erythrocytes. High levels of cell lysis indicated low complement depletion by the surfaces. Data were referenced to water-lyzed erythrocytes (100% lysis control or zero depletion control). Additional control surfaces were also used (e.g., non-tissue culture (TC) plastic and an untreated glass slide). $N = 3$ independent experiments were performed in duplicate wells. $^*p < 0.05$ (compared to the zero depletion control), $+p < 0.05$ (compared to non-TC plastic), $\S p < 0.05$ (compared to untreated glass).

of the PCysMA brush-coated glass slides to human serum, all brushes performed much better with regard to complement depletion than typical non-adherent surfaces (e.g., non-tissue culture plastic and untreated glass, $p < 0.05$). Shorter and intermediate PCysMA brushes (4−7 nm and 13−16 nm dry thicknesses, respectively) led to weak but detectable depletion compared to the zero depletion control ($p < 0.05$). However, the relatively long PCysMA brushes (24−28 nm dry thickness) showed no statistically significant differences compared to the zero depletion control (see Figure 10). These results confirmed the qualitative observations reported in Figure 9B, suggesting that a certain minimum brush thickness is required for optimum antibiofouling performance.[27]

Finally, the complement depletion performance of well-known antibiofouling PMPC and POEGMA brushes was compared to PCysMA brushes of comparable dry thickness (approximately 25−30 nm in each case), see Figure 11.

To maximize the assay sensitivity, complement depletion was monitored over a range of normal human serum (NHS) concentrations (100%, 50%, and 25%), such that the zero depletion controls were still able to completely lyze the cells (see Figure 11B). PCysMA brushes proved to be slightly superior to the PMPC and POEGMA brushes in their antibiofouling properties over the entire concentration range (Figure 11A). The former brushes exhibited no discernible difference compared to the zero depletion control, whereas the PMPC and POEGMA brushes each showed a small but significant increase in complement depletion ($p < 0.05$).

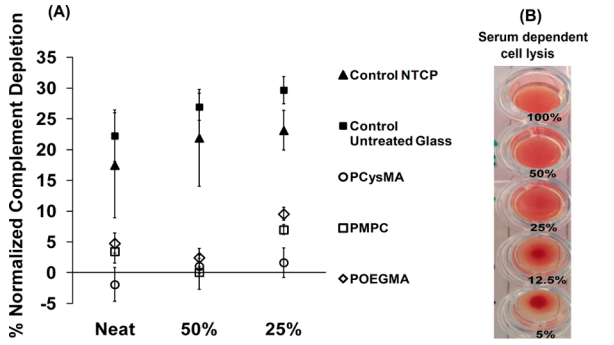

Figure 11. Comparative complement depletion assays for three types of antibiofouling polymer brushes. (a) PCysMA, PMPC and POEGMA brushes of equivalent thickness (approximately 25−30 nm) were tested for complement depletion and data were compared to both non-tissue culture plastic control (NTCP) and untreated glass. Antibiofouling performance was monitored over a range of human serum concentrations (100%, 50%, and 25% serum). Lower concentrations incurred errors because there were insufficient complement proteins to lyze the cells, as shown in part b. (b) $N = 3$ independent experiments were performed in duplicate wells. $^*p < 0.05$ (compared to a zero depletion control).

CONCLUSIONS

A new amino acid methacrylate monomer, cysteine methacrylate (CysMA), has been conveniently prepared on a 40-g scale without recourse to protecting group chemistry via a facile high-yielding thia-Michael addition conducted in aqueous solution, offering the prospect of straightforward and cost-effective scale-up. This monomer was used to prepare novel zwitterionic PCysMA brushes via surface-initiated atom transfer radical polymerization with mean brush thicknesses ranging between 4 and 28 nm. Such brushes exhibit complex pH-responsive behavior. For example, the mean brush thickness increased significantly below pH 2 and above pH 9.5, as judged by ellipsometry and AFM studies. Surface zeta potential studies indicate that PCysMA brushes acquire cationic character below the former pH and anionic character above the latter pH, with zwitterionic character being observed at intermediate pH. Modest brush swelling occurs in the presence of added salt at pH 6, which is attributed to the well-known "antipolyelectrolyte effect" exhibited by polybetaines. In contrast, conventional polyelectrolyte behavior, i.e., brush collapse, is observed on addition of salt at either low pH or high pH, since the electrostatic repulsive forces between adjacent charged chains are screened. XPS studies of photodegraded PCysMA brushes confirm that surface aldehyde groups are generated after prolonged UV irradiation at 244 nm. Both micro- and nanostructured PCysMA brushes can be conjugated to either green fluorescent protein (GFP) via these surface aldehyde groups. PCysMA brushes proved to be highly resistant to adhesion when exposed to HDF cells, while complement consumption/depletion assays confirm that such brushes exhibit superior antibiofouling performance to that of well-known PMPC and POEGMA brushes. Finally, these PCysMA brushes exhibit good long-term stability under physiological conditions, but are prone to base-catalyzed hydrolysis when immersed in mildly alkaline solution (pH > 8).

dx.doi.org/10.1021/ja503400r | J. Am. Chem. Soc. 2014, 136, 9404−9413

■ ASSOCIATED CONTENT

Supporting Information

Experimental section, together with additional experimental data including XPS measurements for BIBB-APTES-functionalized silicon wafers; surface zeta potential measurements for APTES and BIBB-APTES; PCysMA brush surface roughness, change in brush thickness, and XPS data for PCysMA brushes after chemical degradation; fluorescence image for non-patterned PCysMA brushes after protein immobilization; brush disinfection and bioburden assay protocols; details of synthesis of PMPC and POEGMA control brushes; and details of complement consumption/depletion assays. This material is available free of charge via the Internet at http://pubs.acs.org.

■ AUTHOR INFORMATION

Corresponding Authors

graham.leggett@shef.ac.uk
s.p.armes@shef.ac.uk

Present Address

[‖]Institut Charles Gerhardt de Montpellier (UMR 5253, ENSCM-CNRS-UM2) ENSCM, 8, Rue de l'École Normale, 34296 Montpellier, France.

Notes

The authors declare no competing financial interest.

■ ACKNOWLEDGMENTS

The Saudi Arabian government is thanked for funding a Ph.D. studentship for A.M.A. G.J.L. thanks EPSRC for a Programme Grant (EP/I012060/1). S.P.A. acknowledges the ERC for an *Advanced Investigator* Grant (PISA 320372) and EPSRC for a Platform Grant (EP/J007846/1).

■ REFERENCES

(1) Meyers, S. R.; Grinstaff, M. W. *Chem. Rev.* **2011**, *112*, 1615.
(2) Langer, R.; Tirrell, D. A. *Nature* **2004**, *428*, 487.
(3) Lewis, A.; Tolhurst, L.; Stratford, P. *Biomaterials* **2002**, *23*, 1697.
(4) Vlastarakos, P. V.; Nikolopoulos, T. P.; Korres, S.; Tavoulari, E.; Tzagaroulakis, A.; Ferekidis, E. *Eur. J. Pediatr.* **2007**, *166*, 385.
(5) Chan, M. Y.; Weitz, J. I.; Merhi, Y.; Harrington, R. A.; Becker, R. C. *J. Thromb. Thrombolysis* **2009**, *28*, 366.
(6) Jiang, S.; Cao, Z. *Adv. Mater.* **2010**, *22*, 920.
(7) Lundqvist, M.; Stigler, J.; Elia, G.; Lynch, I.; Cedervall, T.; Dawson, K. A. *Proc. Natl. Acad. Sci. U.S.A.* **2008**, *105*, 14265.
(8) Thissen, H.; Gengenbach, T.; du Toit, R.; Sweeney, D. F.; Kingshott, P.; Griesser, H. J.; Meagher, L. *Biomaterials* **2010**, *31*, 5510.
(9) Kodjikian, L.; Burillon, C.; Chanloy, C.; Bostvironnois, V.; Pellon, G.; Mari, E.; Freney, J.; Roger, T. *Invest. Ophthalmol. Visual Sci.* **2002**, *43*, 3717.
(10) Ratner, B. D. *J. Biomed. Mater. Res.* **1993**, *27*, 837.
(11) Harris, J. M. *Poly (Ethylene Glycol) Chemistry: Biotechnical and Biomedical Applications*; Springer: New York, 1992.
(12) Webster, R.; Didier, E.; Harris, P.; Siegel, N.; Stadler, J.; Tilbury, L.; Smith, D. *Drug Metab. Dispos.* **2007**, *35*, 9.
(13) Arima, Y.; Toda, M.; Iwata, H. *Biomaterials* **2008**, *29*, 551.
(14) Senaratne, W.; Andruzzi, L.; Ober, C. K. *Biomacromolecules* **2005**, *6*, 2427.
(15) Lavanant, L.; Pullin, B.; Hubbell, J. A.; Klok, H. A. *Macromol. Biosci.* **2010**, *10*, 101.
(16) Ladd, J.; Zhang, Z.; Chen, S.; Hower, J. C.; Jiang, S. *Biomacromolecules* **2008**, *9*, 1357.
(17) Edmondson, S.; Osborne, V. L.; Huck, W. T. *Chem. Soc. Rev.* **2004**, *33*, 14.
(18) Barbey, R.; Lavanant, L.; Paripovic, D.; Schüwer, N.; Sugnaux, C.; Tugulu, S.; Klok, H.-A. *Chem. Rev.* **2009**, *109*, 5437.
(19) Hawker, C. J.; Bosman, A. W.; Harth, E. *Chem. Rev.* **2001**, *101*, 3661.
(20) Baum, M.; Brittain, W. J. *Macromolecules* **2002**, *35*, 610.
(21) Husseman, M.; Malmström, E. E.; McNamara, M.; Mate, M.; Mecerreyes, D.; Benoit, D. G.; Hedrick, J. L.; Mansky, P.; Huang, E.; Russell, T. P. *Macromolecules* **1999**, *32*, 1424.
(22) Patten, T. E.; Matyjaszewski, K. *Adv. Mater.* **1998**, *10*, 901.
(23) Matyjaszewski, K.; Xia, J. *Chem. Rev.* **2001**, *101*, 2921.
(24) Pyun, J.; Kowalewski, T.; Matyjaszewski, K. *Macromol. Rapid Commun.* **2003**, *24*, 1043.
(25) Perruchot, C.; Khan, M.; Kamitsi, A.; Armes, S. v.; Von Werne, T.; Patten, T. *Langmuir* **2001**, *17*, 4479.
(26) Chen, M.; Briscoe, W. H.; Armes, S. P.; Klein, J. *Science* **2009**, *323*, 1698.
(27) Feng, W.; Brash, J. L.; Zhu, S. *Biomaterials* **2006**, *27*, 847.
(28) Hucknall, A.; Rangarajan, S.; Chilkoti, A. *Adv. Mater.* **2009**, *21*, 2441.
(29) Ma, H.; Wells, M.; Beebe, T. P.; Chilkoti, A. *Adv. Funct. Mater.* **2006**, *16*, 640.
(30) Topham, P. D.; Howse, J. R.; Crook, C. J.; Parnell, A. J.; Geoghegan, M.; Jones, R. A.; Ryan, A. J. *Polym. Int.* **2006**, *55*, 808.
(31) Fielding, L. A.; Edmondson, S.; Armes, S. P. *J. Mater. Chem.* **2011**, *21*, 11773.
(32) Stuart, M. A. C.; Huck, W. T.; Genzer, J.; Müller, M.; Ober, C.; Stamm, M.; Sukhorukov, G. B.; Szleifer, I.; Tsukruk, V. V.; Urban, M. *Nat. Mater.* **2010**, *9*, 101.
(33) Dai, X.; Zhou, F.; Khan, N.; Huck, W. T. S.; Kaminski, C. F. *Langmuir* **2008**, *24*, 13182.
(34) Wu, T.; Gong, P.; Szleifer, I.; Vlček, P.; Šubr, V.; Genzer, J. *Macromolecules* **2007**, *40*, 8756.
(35) Ayres, N.; Boyes, S. G.; Brittain, W. J. *Langmuir* **2007**, *23*, 182.
(36) Parnell, A. J.; Martin, S. J.; Jones, R. A.; Vasilev, C.; Crook, C. J.; Ryan, A. J. *Soft Matter* **2009**, *5*, 296.
(37) Edmondson, S.; Vo, C.-D.; Armes, S. P.; Unali, G.-F. *Macromolecules* **2007**, *40*, 5271.
(38) Chen, S.; Zheng, J.; Li, L.; Jiang, S. *J. Am. Chem. Soc.* **2005**, *127*, 14473.
(39) Zhang, Z.; Chao, T.; Chen, S.; Jiang, S. *Langmuir* **2006**, *22*, 10072.
(40) Yang, W.; Chen, S.; Cheng, G.; Vaisocherová, H.; Xue, H.; Li, W.; Zhang, J.; Jiang, S. *Langmuir* **2008**, *24*, 9211.
(41) Feng, W.; Zhu, S.; Ishihara, K.; Brash, J. L. *Langmuir* **2005**, *21*, 5980.
(42) Zhang, Z.; Chen, S.; Jiang, S. *Biomacromolecules* **2006**, *7*, 3311.
(43) Calvo, A.; Yameen, B.; Williams, F. J.; Soler-Illia, G. J.; Azzaroni, O. *J. Am. Chem. Soc.* **2009**, *131*, 10866.
(44) Liu, Q.; Singh, A.; Liu, L. *Biomacromolecules* **2012**, *14*, 226.
(45) Rosen, J. E.; Gu, F. X. *Langmuir* **2011**, *27*, 10507.
(46) Sundaram, H. S.; Ella-Menye, J.-R.; Brault, N. D.; Shao, Q.; Jiang, S. *Chem. Sci.* **2014**, *5*, 200.
(47) Chan, J. W.; Hoyle, C. E.; Lowe, A. B.; Bowman, M. *Macromolecules* **2010**, *43*, 6381.
(48) Ahmad, S. A.; Leggett, G. J.; Hucknall, A.; Chilkoti, A. *Biointerphases* **2011**, *6*, 8.
(49) Lin, N.; Payer, D.; Dmitriev, A.; Strunskus, T.; Wöll, C.; Barth, J. V.; Kern, K. *Angew. Chem., Int. Ed.* **2005**, *44*, 1488.
(50) Cavalleri, O.; Gonella, G.; Terreni, S.; Vignolo, M.; Floreano, L.; Morgante, A.; Canepa, M.; Rolandi, R. *Phys. Chem. Chem. Phys.* **2004**, *6*, 4042.
(51) Alswieleh, A. M.; Cheng, N.; Leggett, G. J.; Armes, S. P. *Langmuir* **2014**, *30*, 1391.
(52) Dewick, P. M. *Essentials of Organic Chemistry: For Students of Pharmacy, Medicinal Chemistry and Biological Chemistry*; Wiley: New York, 2006.
(53) Dong, R.; Lindau, M.; Ober, C. K. *Langmuir* **2009**, *25*, 4774.
(54) Kumar, M.; Grzelakowski, M.; Zilles, J.; Clark, M.; Meier, W. *Proc. Natl. Acad. Sci. U.S.A.* **2007**, *104*, 20719.
(55) Corbett, J. C. W.; McNeil-Watson, F.; Jack, R. O.; Howarth, M. *Colloids Surf., A* **2012**, *396*, 169.

(56) Lee, H.; Pietrasik, J.; Sheiko, S. S.; Matyjaszewski, K. *Prog. Polym. Sci.* **2010**, *35*, 24.
(57) Brueck, S. *Proc. IEEE* **2005**, *93*, 1704.
(58) Engberg, A. E.; Rosengren-Holmberg, J. P.; Chen, H.; Nilsson, B.; Lambris, J. D.; Nicholls, I. A.; Ekdahl, K. N. *J. Biomed. Mater. Res., Part A* **2011**, *97*, 74.
(59) Yang, W.; Zhang, L.; Wang, S.; White, A. D.; Jiang, S. *Biomaterials* **2009**, *30*, 5617.
(60) Vonarbourg, A.; Passirani, C.; Saulnier, P.; Benoit, J.-P. *Biomaterials* **2006**, *27*, 4356.
(61) Frisch, S. M.; Ruoslahti, E. *Curr. Opin. Cell Biol.* **1997**, *9*, 701.